OPTOELECTRONICS AND ADVANCED MATERIALS – RAPID COMMUNICATIONS Vol. 2, No. 5, May 2008, p. 278 - 283

Raman, SERS and DFT investigations of two metal-chelating compounds

N. LEOPOLD, V. CHIŞ, I.B. COZAR, L. SZABÓ, A. PÎRNĂU, O. COZAR*
Babeş-Bolyai University, Faculty of Physics, Kogălniceanu 1, 400084 Cluj-Napoca, Romania

Raman spectra of 5,5′-nitrilodibarbituric acid (Murexide) and 4-(2-pyridylazo) resorcinol (PAR) metal chelating molecules, were recorded in solid state. Complete assignments of experimental spectra were made by using the B3LYP/6-31G(d) theoretical results. The calculated molecular electrostatic potential of the two compounds shows that for Murexide, the most negative regions are associated with the six oxygen atoms, while for PAR it is associated with the two oxygen and the three nitrogen atoms. Raman and SERS analysis, coupled with DFT results show that Murexide is adsorbed to the silver surface through the N7 atom, while the adsorption of PAR is realized through the N4 atom. Differentiation between PAR- Zn(II), Cu(II) and Fe(III) complexes is shown by the SERS spectral features of each PAR-metal complex, whereas a selective behavior of the silver particles for the Murexide-Zn(II) complex was observed.

(Received March 22, 2008; accepted April 14, 2008)

Keywords: Metal chelating agent, Raman spectra, SERS, DFT

1. Introduction

The molecular recognition property is very important for many biological processes and generally for life [1-5]. Molecular recognition can be carried out by super-molecules with saturated covalent bonds, forming molecular complexes based on the principles of molecular complementarity and held together by intermolecular forces. An essential condition for life is that molecules recognize each other, leading to the formation of some complex combinations with different metabolic roles.

An interesting class of molecules with cationic recognition properties, like deferoxamine (DFO), ethylenediaminetetraacetic acid (EDTA), dimercaptosuccinic acid (DMSA), 2,3-dimercapto-1-propanesulfonic acid (DMPS) or alpha lipoic acid (ALA) are used in conventional and alternative medicine for detoxing the human body of toxic metals, within the so-called *chelation therapy* [6-11]. The chelating agents contain usually donor atoms like nitrogen, oxygen or sulfur which have available electrons to form coordination compounds with a metal ion. While mobilization of the toxic metal out of the body is an important part of *chelation therapy*, the ultimate goal is a decrease in toxicity. The chelate (chelating agent – metal ion complex), has often different properties with respect the chelating agent itself, or the metal ion alone, being usually without toxicity. Chelation therapy consists in the administration of chelating agents to remove heavy metals from the body. The chelating agents bond the metallic ions present in excess in the human body, being afterwards eliminated. Thus, deferoxamine (DFO) shows highest affinity for Fe(III) ions, but it is used also in detoxing processes with Al(III) [2, 4, 8]. EDTA forms stable compounds with bivalent and trivalent ions like Cu(II), Cd(II), Pb(II), Mn(II), Fe(III) and Co(II) [10–15].

In this work, experimental and theoretical investigations on 5,5′-nitrilodibarbituric acid mono-ammonium (Murexide) and 4-(2-pyridylazo) resorcinol (PAR) are presented. Murexide is used in analytical chemistry as a complexometric indicator, most often of Ca(II) ions, but also for Cu(II), Ni(II), Co(II) and rare earth metals. PAR represents also a widely used metal indicator. Recently, a sensor approach for Cu(II) detection in urine, using PAR as chelating agent was reported [16]. The determination of copper in urine is of particular interest in clinical chemistry for purposes of diagnosis, for monitoring Wilson's patients under chelation therapy, for detection of environmental or occupational exposure, and for nutritional studies. Also, an optical sensor for analysis of Zn(II) in pharmaceuticals was developed using PAR as chelating agent [17].

2. Experimental

5,5′-Nitrilodibarbituric acid monoammonium salt (Murexide) and 4-(2-pyridylazo) resorcinol monosodium salt monohydrate (PAR) of the highest commercially available purity were obtained from Merck Romania. Zn(II), Fe(III) and Cu(II) complexes were prepared by adding 0.6 M $ZnCl_2$, $FeCl_3$ and $CuSO_4$ solution aliquots to 0.02 M Murexide and PAR solutions, obtaining the 1:2 ligand:metal ion stoichiometric ratios.

For SERS measurements, 5 μl of analyte were added to 0.5 ml silver colloid. The silver colloidal SERS substrate was prepared reducing silver with hydroxylamine [18]. Briefly, 0.017 g silver nitrate were solved in 90 ml distilled water. In a separate recipient, 0.017 g of

hydroxylamine hydrochloride were solved in 10 ml water, followed by the addition of 0.17 ml sodium hydroxide solution 2 mol/l. The hydroxylamine/sodium hydroxide solution was then added rapidly to the silver nitrate solution under vigorous stirring. After a few seconds a grey brown colloidal solution resulted, with pH value 8.5, and was further stirred for 10 minutes. SERS spectra were recorded with a Raman Microspectrometer LabRam HR800 (Jobin Yvon) equipped with a coupled charge detector (CCD) and a HeNe laser emitting at 632.8 nm with power set to 14.5 mW. All SERS spectra were recorded with a spectral resolution of about 4 cm^{-1}. FT-Raman spectra of powder samples were recorded in backscattering geometry with a FRA 106/S (Bruker) Raman accessory equipped with nitrogen cooled Ge detector. The 1064 nm Nd:YAG laser was used as excitation source, and the laser power was set at 400 mW. All spectra were recorded with a resolution of about 4 cm^{-1} by co-adding 32 scans.

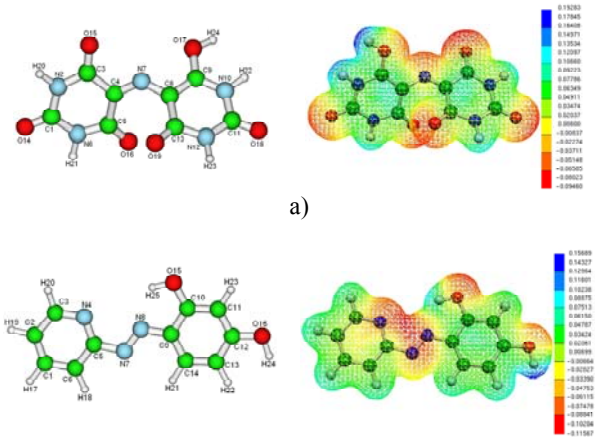

a)

b)

Fig. 1. Optimized geometries and the calculated 3D molecular electrostatic potentials for Murexide (a) and PAR (b).

3. Computational details

The molecular geometry optimizations, vibrational spectra and molecular electrostatic potential calculations were performed with the Gaussian 98W software package [19] by using Density Functional Theory (DFT) methods with B3LYP hybrid exchange-correlation functional [20-22] and the standard 6-31G(d) basis set. The geometries were fully optimized without any constraint with the help of analytical gradient procedure implemented within Gaussian 98W program. The vibrational frequencies were computed at the optimized geometry to ensure that no imaginary frequencies were obtained, confirming that it corresponds to a local minimum on the potential energy surface. Vibrational mode assignments were made by visual inspection of modes animated by using the Molekel program [23].

4. Results and discussion

Adsorption to the silver surface

The optimized geometries and the 3D molecular electrostatic potential (MEP) contour map are shown in Fig. 1. The MEP is widely used as such a reactivity map displaying most probable regions for the electrophilic attack and in studies of biological recognition and hydrogen bonding interactions [24]. As can be seen in the MEP distributions, negative V(r) values for the Murexide molecule are associated with O14, O15, O16, O17, O18, O19 and N7 atoms. Calculations reveal that the most negative values correspond to the nitrogen atom, with a value around -0.094a.u. Thus, it would be predicted that an electrophile will preferentially attack Murexide at the N7 site. For PAR, negative regions are associated with N4, N7, N8, O15 and O16 atoms. Also, it must be considered that, when added to the silver colloidal solution, the chlorine anions chemisorbed onto the colloidal surface induce positively Ag charged particles [25, 26], and thus, the adsorption of the molecules to the silver surface is supposed to occure through atoms with high negative charges. In addition, the adsorption through the ring π-electrons is not sustained by the MEP distribution.

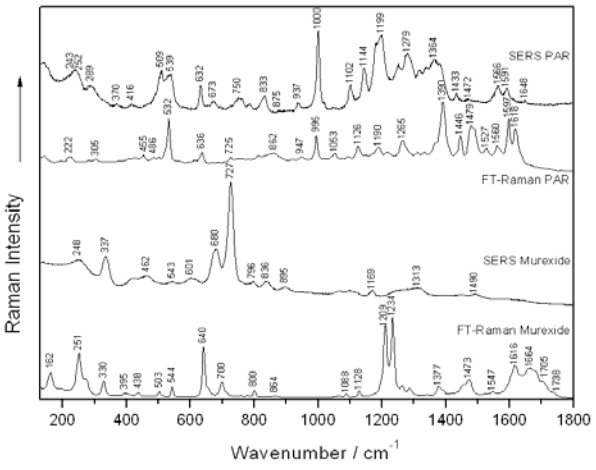

Fig. 2. FT-Raman and SERS spectra of Murexide and PAR.

After the optimization of the molecular geometries, the normal vibrational modes of the Murexide and PAR molecules were calculated and some selected bands are collected in Tables 1 and 2. The calculated wavenumbers were scaled with the 0.9614 factor, corresponding to the B3LYP / 6-31G(d) method [27].

Table 1. The assignment of Raman bands for Murexide.

Mode	Experimental wavenumbers (cm^{-1})	Calculated wavenumbers (cm^{-1})	Assignments
1	162	175	γ rings
2	251	248	γ rings
3	330	311	γ rings
4	395	398	δ(CCO)+δ(NCO)
5	438	434	γ(CN)+γ(NH)
6	503	499	δ(NCC)+δ(CNC)+δ(CCN)
7	544	530	δ(CCN)+δ(CNC)
8	640	653	rg 2 breathing+γ(NH)
9	700	710	δ(CCO)+δ(NCO)
10	800	804	τ(CC) +τ(CN)
11	1209	1201	υ(CN)+in plane rings def.
12	1234	1230	ν(CN)+δ(OH)
13	1377	1376	ν(N6C1N2)+δ(NH)
14	1473	1475	υ(C9N10)
15	1616	1628	ν(C8C9)+ν(C4N7)

ν-stretching, δ-in plane bending, τ-twisting, γ-out of plane bending, rg2-C8-C9-N10-C11-N12-C13

Table 2. The assignment of Raman bands for PAR.

Mode	Experimental wavenumbers (cm^{-1})	Calculated wavenumbers (cm^{-1})	Assignments
1	222	217	γ(rg2)+γ(NN)
2	532	530	i.p. rg2 def.
3	636	633	i.p. rg1 def.
4	862	855	τ(CH)
5	995	1007	δ(CCC rg1)+δ(CNC rg1)
6	1053	1030	δ(CCC rg1)
7	1126	1132	δ(CH rg1)
8	1190	1186	δ(OH)+δ(CH)+ν(CN)
9	1265	1249	ν(CC)+ν(CN)+δ(CH)
10	1390	1417	δ(CH)+ν(CC)
11	1446	1435	ν(NN)+ν(CC)+δ(CH)
12	1479	1486	υ(NN)+δ(CH)
13	1560	1567	ν(CC)+ν(CN)+δ(CH)
14	1597	1579	υ(CC)+δ(CH)
15	1618	1618	υ(CC)+δ(CH)

ν-stretching, δ-in plane bending, τ-twisting, γ-out of plane bending, rg1- C1-C2-C3-N4-C5-C6, rg2-C9-C10-C11-C12-C13-C14

The FT-Raman and SERS spectra of Murexide and PAR molecules are shown in Fig. 2. The assignments of the most intense bands in the Raman spectra of the two molecules are given in Tables 1 and 2, respectively.

As discussed previously, DFT calculations predict the highest most negative values of the MEP for Murexide molecule on the oxygen atoms and the N7 nitrogen atom. Therefore, most probably, these atoms will be involved in the molecule absorption to the colloidal Ag surface. By comparing the SERS and Raman spectra of Murexide (Figure 2), some major differences can be noticed. Thus, the most enhanced SERS bands are those from 680 and 727 cm^{-1}, while the Raman bands from 1209 and 1234 cm^{-1} and those around the value of 1600 cm^{-1}, which are among the most intense bands from the Murexide Raman spectrum, do not appear in the SERS spectrum. All these changes clearly indicate an interaction between Murexide molecules and Ag particles. However, binding of the molecule by one of the oxygen atoms is excluded because this would involve the enhancement in the SERS spectrum of the bands corresponding to the vibrations involving CO group. As seen in Fig. 2, these bands appear at about 1664, 1705 and 1738 cm^{-1}. In addition, the bands related to the stretching vibrations of the ring CC and CN bonds should be enhanced, according to the SERS selection rules.

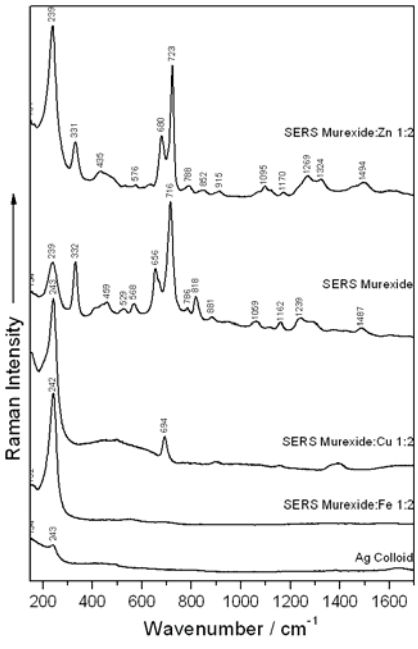

Fig. 3. SERS spectra of Murexide and Murexide-metal complexes prepared with the corresponding metal salt, at the stoichiometric ratios indicated in the figure. Raman spectrum of the silver colloid is also shown for comparison.

Consequently, the adsorption of the molecule through the nitrogen N7 atom is plausible and the arguments in favor of this hypothesis will be presented bellow. If the molecule is bound to the Ag surface through the N7 atom and taking into account that the molecule is not planar, the out of plane bending vibrations, but also stretchings of the two rings should be amplified according to the same SERS

selection rules. Analyzing the SERS spectrum and considering the assignments given in Table 1, we can notice that SERS bands at 337 cm^{-1}, 462 cm^{-1}, 680 cm^{-1} and 727 cm^{-1} are enhanced. In addition, the disappearance of the bands around 1234 cm^{-1}, corresponding to in-plane ring deformation vibrations confirms this hypothesis.

In case of PAR molecule, the DFT calculated electrostatic molecular potential indicates the fact that the highest electronic density is distributed around the nitrogen and oxygen nuclei. Therefore, the adsorption of the PAR molecule to the Ag colloidal particles surface is possible by these atoms.

Comparing the Raman and SERS spectra of PAR in Figure 2, it can be noticed that the position and the relative intensity modification of several bands, indicate the existence of an interaction between the PAR molecule and the Ag particles. The most intense SERS bands are those around the values 509, 632, 1000, 1199 and 1364 cm^{-1}, while in the Raman spectrum the most intense bands appear around the values of 532, 935, 1390, 1479, 1597 and 1618 cm^{-1}. Taking into account the optimized geometry of the PAR molecule, we consider that the adsorption through the N7 and N8 atoms is less probable due to sterical (geometrical) reasons. The adsorption through the N7 and N8 atoms is also improbable, because in the case of the existence of this bonding type, the vibration of the NN bond should appear amplified in the SERS spectrum, but in reality this band (1479 cm^{-1}) is very weak. Therefore, the most probable way of PAR adsorption to the Ag surface is through the N4 atom, the spectral modifications which appear in the SERS spectrum, compared to the Raman spectrum, confirming this way of adsorption.

The enhancement of the PAR SERS bands at 539 cm^{-1} and 632 cm^{-1} assigned to in plane deformation vibrations of the two rings, sustain the hypothesis of adsorption of PAR through the N4 atom. Also, the bands at 1199 cm^{-1} and 1364 cm^{-1}, which are enhanced in the SERS spectrum of PAR, assigned to in plane deformation modes of the molecule (Table 2.), confirm this supposition.

Taking in account the SERS selection rules and the amplification of the vibrations due to several stretching or deforming vibrations in the molecule plane, it can be concluded that the adsorbed PAR molecule is orientated rather perpendicular on the metallic surface.

In general, the bands attributed to the total symmetrical vibrations of the aromatic rings appear in the Raman spectra as bands of medium or high intensity being, normally, very narrow. For PAR molecule, the total symmetric vibrations of the two aromatic rings can be seen in Raman spectrum at 532 and 995 cm^{-1}, respectively. The corresponding bands appear amplified in the SERS spectrum at 539 and 1000 cm^{-1}, respectively. Therefore a tilted orientation on the metallic Ag surface is expected for PAR molecule.

Murexide and PAR metal compounds.

The molecular electrostatic potential can also be useful for predicting the possible coordination sites of a given molecule when it forms molecular complexes containing different metallic ions. As previously reported [28-32], when forming 2:1 complexes with Cu(II), Zn(II) or Cd(II), metal ions are bonded by the O15-N7-O17 atom group of Murexide. Also, 1:1 Murexide complexes with Ca(II) and Ni(II) were reported in the literature [33-35]. We investigated the adsorbtion of Murexide-metal complexes, with Fe, Cu and Zn. SERS spectra of the investigated complexes are given in Fig.3. As seen in this figure, only the Murexide-Zn(II) complex shows adsorption affinity to the silver surface, leading to successfully recording of the SERS spectrum. The shift of the 716 cm^{-1} SERS band of Murexide to 723 cm^{-1} in the SERS spectrum of the Murexide-Zn(II) complex is attributed to the changes in the molecular structure due to the formation of the Zn(II) complex. The complexes of Murexide with Fe(III) and Cu(II) show no adsorption affinity to the silver surface, therefore the SERS spectra, in the presence of these complexes, show only the adsorptions of Cl^- and probably of SO_4^- anions, as indicated by the bands at 242 and 694 cm^{-1}, respectively. Thus, the silver particles present a selective behavior for Murexide-Zn(II) complexes, suggesting the possible development of a Zn(II) sensor using SERS as transducing method and Murexide as chelating agent, without interference from Fe(III) and Cu(II) ions.

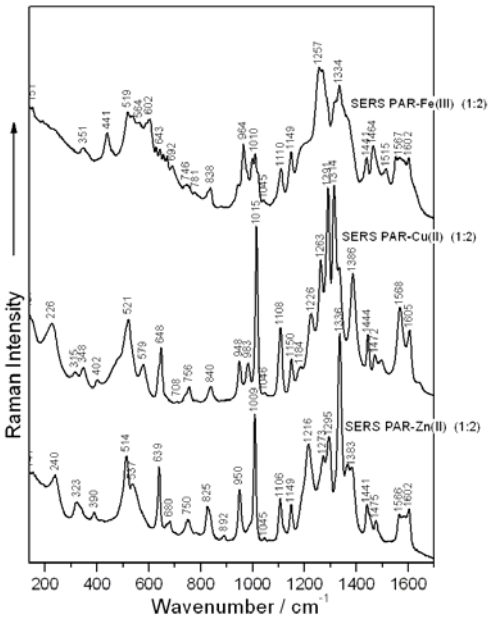

Fig. 4. SERS spectra of PAR- Zn(II), Cu(II) and Fe(III) complexes, prepared at PAR:metal salt 1:2 stoichiometric ratio.

The chelation mode of PAR with some metal ions was reported by Greay *et al*. [36]. At pH values above 5.0, PAR forms 2:1 complexes with Zn(II) and Cu(II) [16], the atoms involved in the coordination being the pyridine nitrogen (N4), the azo nitrogen farthest from the

heterocyclic ring (N8), and the o-hydroxyl group (O15) [37-39].

As seen in Fig. 4 where the SERS spectra of PAR-Zn(II), Cu(II) and Fe(III) complexes are given, PAR-metal complexes can be differentiated by their SERS spectral features. Thus, shifts of band positions and changes in relative intensities in the SERS spectra suggest structural modifications due to the complexation of the Zn(II), Fe(III) and Cu(II) ions with PAR ligand. Each PAR-metal complex SERS spectrum in Figure 4 shows a characteristic spectral fingerprint. Thus, several SERS bands are representative for each PAR-metal complex: 441, 964, 1257, 1334 and 1464 cm^{-1} for PAR-Fe(III), 648, 1015, 1291, 1314 and 1386 cm^{-1} for PAR-Cu(II) and 514, 639, 1009, 1216 and 1336 cm^{-1} for PAR-Zn(II) complex.

5. Conclusions

Optimized geometries, molecular electrostatic potential and normal modes of Murexide and PAR molecules were calculated by theoretical DFT methods. The assignment of the experimental vibrational bands of these molecules was done on the basis of B3LYP/6-31G(d) theoretical results.

Comparing the Raman and SERS spectra of Murexide and PAR, the atoms involved in the adsorption to the Ag surface, and also the adsorption geometries of the two molecules were derived. Both molecules, Murexide and PAR, are adsorbed in a predominant perpendicular orientation on the Ag surface, Murexide through the N7 atom, whereas PAR through the N4 atom.

The silver particles present a selective behavior for Murexide-Zn(II) complexes, thus showing the potential for developing a Zn(II) sensor using SERS as transducing method and Murexide as chelating agent, without interference from Fe(III) and Cu(II) ions.

PAR- Zn(II), Cu(II) and Fe(III) complexes can be differentiated by their SERS spectral features, each PAR-metal complex SERS spectrum showing a characteristic spectral fingerprint.

Acknowledgment

Financial support from the Romanian National Authority for Scientific Research is highly acknowledged (grant ID 501). The authors are also grateful to dr. Monica Venter for many useful discussions.

References

[1] G. Winkelmann, Handbook of microbial iron chelates, CRC Press, Boca Raton, 1991.
[2] S. Dhunganga, P. S. White, A. L. Crumbliss, J. Biol. Inorg. Chem. **6**, 810 (2001).
[3] Z. Yehuda, Y. Hadar, Y. Chen, J.Agric. Food Chem. **51**, 5996 (2003).
[4] B. Borgias, A. D. Hugi, K. N. Raymond, Inorg Chem. **28**, 3538 (1989).
[5] J. Leong, K. N. Raymond, J. Am. Chem.Soc. **97**, 293 (1975).
[6] D. F. Thompson, E. D.Callen, Ann. Pharmacother. **38**, 1509 (2004).
[7] M. Blanuşa, V. M. Varnai, M. Piasek, K. Kostial, Current Medicinal Chemistry **12**, 2771 (2005).
[8] O. Cozar, N. Leopold, C. Jelic, V. Chiş, L. David, A. Mocanu, M. Tomoia-Cotisel, J. Molec. Structure **1**, 788 (2006).
[9] J. F. Risher, S. N. Amler, Neurotoxicology **26**(4), 691 (2005).
[10] J. S. Shrihari, A. Roy, D. Prabhakaran, K. S. Reddy, Natl. Med. J. India **19**(1), 24 (2006).
[11] D. M. Seely. P. Wu, E. J. Mills, BMC Cardiovascular Disorders **5**(32), (2005).
[12] J. J. Chisolm Jr., Journal of Toxicology - Clinical Toxicology **30**(4), 493, 1992
[13] C. D. Klaasen, The Pharmacological Basis of Therapeutics. 11th Ed.; McGraw – Hill: New York, 2006.
[14] C. L. Seaton, J. Lasman, D. R. Smith, Toxicol. Appl. Pharmacol **153**, 159 (1999).
[15] D. F. Thompon, E. D. Callen, Ann. Pharmacother. **38**, 1509 (2004).
[16] P. C. A. Jeronimo, A. N. Araujo, M. C. B. S. M. Montenegro, C. Pasquini, I. M. Raimundo Jr, Anal. Bioanal. Chem., **108**, 380 (2004).
[17] P. C. A. Jeronimo, A. N. Araujo, M. Conceicao, B. S. M. Montenegro, Sens. Actuators B **103**, 169 (2004).
[18] N. Leopold, B. Lendl, J. Phys. Chem. B, **107**, 5723 (2003)
[19] M. J. Frisch, G. W. Trucks, H. B. Schlegel, G. E. Scuseria, M. A. Robb, J. R. Cheeseman, V. G. Zakrewski, J. A. Montgomery Jr., R. E. Stratmann, J. C. Burant, S. Dapprich, J. M. Millam, A. D. Daniels, K. N. Kudin, M. C. Strain, O.Farkas, J. Tomasi, V. Barone, M. Cossi, R. Cammi, B. Mennucci, C. Pomelli, C. Adamo, S. Clifford, J. Ochterski, G. A. Petersson, P. Y. Ayala, Q. Cui, K. Morokuma, D. K. Malik, A. D. Rabuck, K. Raghavachari, J. B. Foresman, J. Cioslowski, J.V. Ortiz, A.G. Baboul, B.B. Stefanov, G. Liu, A. Liashenko, P. Piskorz, I. Komaromi, R. Gomperts, R. L. Martin, D. J. Fox, T. Keith, M.A. Al-Laham, C.Y. Peng, A. Nanayakkara, C. Gonzalez, M. Challacombe, P.M.W. Gill, B. Johnson, W. Chen, M.W. Wong, J.L. Andres, C. Gonzalez, M. Head-Gordon, E.S. Replogle, J. A. Pople, Gaussian 98, Revision A.7, Gaussian, Inc., Pittsburg, PA, 1998
[20] R. G. Parr, W. Yang, Density-Functional Theory of Atoms and Molecules, Oxford University Press, New York, 1989
[21] A.D. Becke, J.Chem.Phys. **98**, 5648 (1993)
[22] C. Lee, W. Yang, R.G. Parr, Phys.Rev. B, **37**, 785 (1988).

[23] P. Flukiger, H. P. Luhti, S. Portmann, J. Weber, MOLEKEL 4.2, Swiss Center for Scientific Computing, Manno (Switzerland), 2000–2002; S. Portmann, H.P. Luhti, Chimia, **54**, 766 (2000).
[24] P. Politzer, D. G. Truhlar, (Eds.), Chemical Application of Atomic and Molecular Electrostatic Potentials, Plenum, New York, 1981.
[25] M. Muniz-Miranda, G. Sbrana, J. Raman Spectroscop., **27**, 105 (1996).
[26] H. Wetzel, H. Gerischer, Chem. Phys. Lett., **76**, 460 (1980).
[27] A. P. Scott, L. Radom, J. Phys. Chem. **100**, 16502 (1996).
[28] R. L.Martin, A. H. White, A. C. Willis, J.Chem.Soc.,Dalton Trans. 1336 (1977)
[29] D. L. Kepert, A. H. White, A. C. Willis, J. Chem. Soc., Dalton Trans. 1342 (1977)
[30] S. R. Hall, B. W. Skelton, A.H.White, A.C.Willis, J.Chem.Soc., Dalton Trans. 639 (1982).
[31] A. H. White, A. C. Willis J. Chem. Soc., Dalton Trans. 372 (1977).
[32] C.L.Raston, A. H. White, A. C. Willis, J. Chem. Soc., Dalton Trans. 1381 (1977)
[33] H. Abdollahi, F. Nazari, Anal. Chim. Acta **109**, 486 (2003)
[34] K. Grudpan, J. Jakmunee, Y. Vaneesorn, S. Watanesk, U.A. Maung, P. Sooksamiti, Talanta **46**, 1245 (1998)
[35] T. Suzuki, A. Hioki, M. Kurahashi, Anal. Chim. Acta, **159**, 476 (2003)
[36] W. J. Greay, G. Nickless, F. H. Pollard, Anal. Chim. Acta, **27**, 71 (1962)
[37] J. Ghasemi, H. Peyman, M. Meloun, J. Chem. Eng. Data **52**, 1171 (2007)
[38] Z. T. Jiang, J. C. Yu, H. Y. Liu, Anal. Sci., **21**, 851 (2005)
[39] F. Karipcin, E. Kabalcilar, Acta Chim. Slov., **54**, 242 (2007).

*Corresponding author: cozar@phys.ubbcluj.ro